Temporal correlation statistic for intrinsic phase fluctuation in double white dwarf gravitational-wave signals

Naoki Seto

Department of Physics, Kyoto University, Kyoto 606-8502, Japan

(Received 26 February 2026; accepted 11 June 2026; published 8 July 2026)

We present a framework to probe intrinsic stochastic fluctuation in the orbital phase evolution of long-lived double white dwarf binaries through gravitational-wave observations with LISA. To capture the essential structure of the fluctuation, we introduce a minimal quadratic statistic that isolates its temporal correlation. We derive a simple analytic scaling relation for the signal-to-noise ratio of this correlation statistic, explicitly showing its dependence on the total observation time and the intrinsic phase correlation time.

DOI: 10.1103/dcdn-gl9v

I. INTRODUCTION

Space-based gravitational-wave (GW) observatories like LISA will resolve a large population of compact binaries in the millihertz band [1–3]. Among these, double white dwarfs (DWDs) are expected to be particularly abundant, with $\sim 10^4$ systems identified over the nominal four-year mission [4]. Their long-lived, nearly monochromatic signals enable continuous tracking of orbital phase evolution over the observational period $T_{\rm obs} \gtrsim 4$ yr [1].

For such systems, the GW phase provides a direct and well-defined tracer of the binary's orbital motion [5–7]. Unlike electromagnetic observables, the generation of GWs is directly tied to the bulk orbital dynamics and is insensitive to source-specific effects such as viscous heating.

In standard GW analyses of long-lived DWDs, the orbital phase evolution is modeled deterministically using the orbital frequency and its low-order time derivatives (see, e.g., Ref. [8]). At sufficiently high phase measurement precision, however, DWDs in the LISA band may exhibit small deviations from idealized smooth phase evolution [9,10]. Finite-size effects can couple the orbital dynamics to additional physical processes, possibly introducing small phase perturbations beyond deterministic secular evolution. Such departures appear as phase residuals once a deterministic model is applied. Timing observations of the semidetached DWD HM Cancri over multiyear baselines [11,12] may serve as a benchmark for phase stability in interacting systems. While broadly consistent with smooth secular evolution, they do not exclude stochastic phase fluctuation at the level of ~0.1 radians. We therefore ask how sensitively such a fluctuation can be detected in LISA data.

A closely related framework has long been developed in pulsar timing, where deviations from simple deterministic spin-down models are analyzed through correlated timing residuals [13,14]. In that context, the pulse arrival times of neutron stars are tracked over decades, and residual correlations are used to identify stochastic or long-timescale components beyond secular evolution [15]. Such methods have played a central role in nanohertz GW searches [16,17].

The present work adopts a viewpoint similar to pulsar timing, but reformulates it for GW observations of DWDs, where phase information is extracted through template-based matched filtering. We focus on time-domain correlations as a minimal diagnostic of intrinsic stochastic phase fluctuation. Our aim is to establish a transparent baseline for assessing such fluctuation, prior to full covariance or likelihood treatment. Within this framework, we derive a simple analytic scaling relation that clarifies how the sensitivity depends on observation time, total signal-to-noise ratio, and intrinsic correlation timescale.

For concreteness, we adopt a fiducial example consisting of a nearly monochromatic DWD with a GW frequency of 3 mHz, observed over a total duration $T_{\rm obs} = 4$ yr with a matched-filter signal-to-noise ratio $\rho_{\rm tot} = 100$ [1,4].

The structure of this paper is as follows. In Sec. II, we define segment-level phase residuals and the linear operations applied to the data, including polynomial phase projection. In Sec. III, we construct a time-domain correlation statistic and derive its expectation value, variance, and scaling behavior under simple assumptions. The implications for detectability and sensitivity to intrinsic correlation timescales are discussed in Sec. IV, followed by related discussions in Sec. V. Section VI is devoted to a brief summary. The Appendix discusses the effects of polynomial phase fitting in more detail.

II. POLYNOMIAL PHASE FITTING AS A LINEAR PROJECTION

In this section, we clarify that polynomial phase fitting in long-lived GW signals is equivalent to a linear projection acting on the phase fluctuation. This equivalence enables a unified treatment of intrinsic phase fluctuation and detector noise.

A. Setup

We write the observed data stream as

$$d(t) = g(t) + n(t), \tag{1}$$

where $g(t)$ is the GW signal and $n(t)$ denotes detector noise.

We model the GW signal as

$$g(t) = A(t)e^{i[\phi_p(t;\boldsymbol{a}_t)+s(t)]}, \tag{2}$$

where $A(t)$ is a slowly varying amplitude, and $s(t)$ denotes a small intrinsic phase fluctuation satisfying $|s(t)| \ll 1$. The secular phase evolution is described by a low-order polynomial,

$$\phi_p(t;\boldsymbol{a}) = \sum_{m=0}^{p} a_m t^m, \tag{3}$$

where $\boldsymbol{a} = (a_0, \ldots, a_p)$ denote the model parameters, whose true values are $\boldsymbol{a}_t$.

In this paper, we neglect the deterministic annual modulation induced by the detector's orbital motion [1,8,18]. This simplification is made to isolate the analytic scaling of the intrinsic stochastic phase-correlation statistic. In a realistic analysis, the Doppler, amplitude, and polarization modulations produced by the annual motion of LISA should be included in the fitted waveform, or equivalently treated as additional deterministic degrees of freedom in the projection. Residual phase components that overlap with these deterministic response modes can therefore be partially absorbed or distorted by the fit, especially for timescales close to one year. The resulting sensitivity should be calibrated with the full time-dependent LISA response.

B. Fitting with a simplified template

We introduce a simplified template waveform,

$$h(t;\boldsymbol{a}) = A(t)e^{i\phi_p(t;\boldsymbol{a})}, \tag{4}$$

which retains only the secular polynomial phase evolution. The template parameters are obtained by matched filtering the data, and the fitted values are denoted by $\boldsymbol{a}_f$. For a nearly monochromatic signal, the noise spectral density can be approximated as constant across the signal bandwidth. The noise-weighted inner product then reduces, up to normalization, to a simple time-domain integral, rendering the matched-filter problem equivalent to a least-squares fit in the time domain (see, e.g., Ref. [19]). In the present work, we frequently apply this approximation.

Since the template does not model the intrinsic phase fluctuation $s(t)$ and the data contain detector noise, the fitted parameters $\boldsymbol{a}_f$ generally deviate from their true values $\boldsymbol{a}_t$. We define the parameter estimation error as

$$\delta\boldsymbol{a} \equiv \boldsymbol{a}_f - \boldsymbol{a}_t. \tag{5}$$

In the small-fluctuation ($s(t) \ll 1$) and high-signal-to-noise regime ($\rho_{\mathrm{tot}} \gg 1$), the mismatch can be linearized, yielding

$$\delta\boldsymbol{a} = \delta\boldsymbol{a}_s + \delta\boldsymbol{a}_n, \tag{6}$$

where the two terms denote contributions from the intrinsic phase fluctuation and detector noise, respectively.

Expanding the true phase to first order in the parameter estimation error $\delta\boldsymbol{a}$, we have

$$\phi_p(t;\boldsymbol{a}_t) + s(t) \simeq \phi_p(t;\boldsymbol{a}_f) + s'(t) + n'_c(t), \tag{7}$$

where $s'(t) = s(t) - \phi_p(t;\delta\boldsymbol{a}_s)$ denotes the intrinsic phase fluctuation remaining after phase fitting, and $n'_c(t) = -\phi_p(t;\delta\boldsymbol{a}_n)$ is an effective phase contribution induced by detector noise through parameter estimation error [20]. Phase fitting removes from both $s(t)$ and $n(t)$ the components that are degenerate with the polynomial phase model.

This absorption can be viewed as a linear projection onto the subspace orthogonal to low-order polynomial phase variations [20–22]. In the continuous-time formulation, the corresponding expressions become algebraically involved. For clarity, we make this projection structure explicit in the discretized (segment-space) formulation introduced below.

C. Discretization

To obtain a discretized time series that probes the postfit phase residuals appearing in Eq. (7), we introduce a segment-level phase estimator. We divide the data stream into N segments of duration T_{seg} and assign a representative time t_k to each segment $(k = 1, \ldots, N)$.

Using the fitted polynomial-phase template $h(t;\boldsymbol{a}_f)$, we define a segment-level estimator

$$x_k \equiv \frac{\mathrm{Im}(d|h_k(\boldsymbol{a}_f))}{(h_k(\boldsymbol{a}_f)|h_k(\boldsymbol{a}_f))}, \tag{8}$$

where $(\cdot|\cdot)$ denotes the usual noise-weighted inner product and $h_k(\boldsymbol{a}_f)$ is the restriction of the template to segment k (see also Refs. [19,20]). As can be readily verified from a first-order expansion of the complex exponential in Eq. (7), this estimator isolates the phase deviations at leading order. It corresponds to projecting the data onto the quadrature component orthogonal to the fitted template [23].

Under the conditions $s(t) \ll 1$ and $\rho_{\mathrm{tot}} \gg 1$, the segment-level estimator can be written as

$$x_k \simeq s'_k + n'_k. \tag{9}$$

Here

$$s'_k \equiv \frac{(s' h_k(\boldsymbol{a}_f)|h_k(\boldsymbol{a}_f))}{(h_k(\boldsymbol{a}_f)|h_k(\boldsymbol{a}_f))} \tag{10}$$

denotes the contribution from the intrinsic phase fluctuation.

In Eq. (9), the noise contribution is given by

$$n'_k = n_k + n'_{c,k}, \tag{11}$$

where the direct detector-noise term and the fitting-induced contribution are defined as

$$n_k \equiv \frac{\mathrm{Im}(n|h_k(\boldsymbol{a}_f))}{(h_k(\boldsymbol{a}_f)|h_k(\boldsymbol{a}_f))}, \tag{12}$$

$$n'_{c,k} \equiv \frac{(n'_c h_k(\boldsymbol{a}_f)|h_k(\boldsymbol{a}_f))}{(h_k(\boldsymbol{a}_f)|h_k(\boldsymbol{a}_f))}. \tag{13}$$

By construction, s'_k and n'_k represent the intrinsic and detector-noise contributions to the phase estimate x_k in segment k. In Eq. (9), they are not separately observable; rather, they constitute a decomposition of the single measured quantity x_k into physically distinct contributions. This decomposition clarifies the two origins of the segment-level phase deviations and provides a convenient basis for the statistical analysis developed below.

We also define

$$s_k \equiv \frac{(s h_k(\boldsymbol{a}_f)|h_k(\boldsymbol{a}_f))}{(h_k(\boldsymbol{a}_f)|h_k(\boldsymbol{a}_f))} \tag{14}$$

as the segment-level contribution associated with the original fluctuation $s(t)$.

D. Evaluation of the intrinsic contribution

Next we explicitly evaluate the intrinsic contribution s'_k introduced above. From Eqs. (7) and (10), this quantity provides a discretized description of the intrinsic phase fluctuation after polynomial phase fitting.

When the segment duration satisfies $T_{\mathrm{seg}} \ll 1$ yr, variations in the signal amplitude $A(t)$ on annual timescales can be neglected. In this regime, the intrinsic contribution reduces to a simple time average of the postfit residual phase over each segment,

$$s'_k \simeq \frac{1}{T_{\mathrm{seg}}} \int_{\mathrm{segment}\,k} s'(t) dt. \tag{15}$$

This relation provides the leading-order mapping from the continuous-time intrinsic fluctuation $s'(t)$ to the discretized time series used in the subsequent analysis. An analogous expression holds for s_k, defined in terms of the original fluctuation $s(t)$.

For compact notation, we collect the segment-level intrinsic contributions into vector form,

$$\boldsymbol{s}' \equiv (s'_1, s'_2, \ldots)^{\mathsf{T}}, \qquad \boldsymbol{s} \equiv (s_1, s_2, \ldots)^{\mathsf{T}}. \tag{16}$$

The effect of polynomial phase fitting on the intrinsic fluctuation can be expressed as a linear operation in the segment space (see, e.g., Refs. [14,17]). Let X denote the design matrix whose columns are given by the polynomial basis functions evaluated at the representative segment times t_k,

$$X_{km} = t_k^m, \quad m = 0, 1, \ldots, p. \tag{17}$$

In this representation, the intrinsic fluctuation sequence after phase fitting is given by

$$\boldsymbol{s}' = P\boldsymbol{s}, \tag{18}$$

with the projection operator [14,17]

$$P = I - X(X^{\mathsf{T}}X)^{-1}X^{\mathsf{T}}. \tag{19}$$

This projection structure is equivalent to the standard linear estimator associated with polynomial parameter fitting and is closely related to the Fisher-matrix formulation in the high-SNR limit (see, e.g., Ref. [20]). It removes components of $\boldsymbol{s}$ that are degenerate with the polynomial phase model, retaining only fluctuation beyond smooth secular trends.

E. Detector noise contribution

We now consider the contribution of detector noise to the segment-level phase estimator, $n'_k = n_k + n'_{c,k}$ [cf. Eqs. (12) and (13)].

Analogously to Eq. (15), the fitting-induced noise contribution can be approximated as

$$n'_{c,k} \simeq \frac{1}{T_{\mathrm{seg}}} \int_{\mathrm{segment}\,k} n'_c(t) dt. \tag{20}$$

It is convenient to collect the noise-related quantities into vector form,

$$\boldsymbol{n}' \equiv (n'_1, n'_2, \ldots)^{\mathsf{T}}, \qquad \boldsymbol{n} \equiv (n_1, n_2, \ldots)^{\mathsf{T}}. \tag{21}$$

In the discretized representation, we find that the effect of phase fitting on detector noise can again be written as a linear operation,

$$\boldsymbol{n}' = P\boldsymbol{n}, \tag{22}$$

where $\boldsymbol{n}'$ denotes the noise contribution after polynomial phase fitting, and P is the same projection operator defined previously.

Formally, Eqs. (18) and (22) take a compact form as if the data were first discretized into segment-level quantities and subsequently projected by the operator P. It should be stressed, however, that this interpretation does not reflect the actual order of operations in the derivation. In practice, we evaluate the effect of parameter-estimation errors within the continuous-time matched-filtering framework, and construct the segment-level estimators only afterward, under standard linearization and discretization approximations. Projection representations (18) and (22) therefore provide a convenient linear description of the final result, rather than a shortcut in the derivation. At linear order, this rearrangement is justified by the fact that discretization through inner products and the projection induced by phase fitting are both linear operations and hence commute, leading to equivalent results irrespective of the order in which they are applied.

III. STATISTICAL STRUCTURE OF PROJECTED PHASE RESIDUALS

In this section, we characterize the correlation structure of the segment-level projected phase residuals, for both detector noise n'_k and intrinsic phase fluctuation s'_k.

This comparison clarifies their statistical distinction, which underlies the nondiagonal correlation statistic introduced in the next section.

A. Detector-noise correlations before and after projection

We first evaluate the covariance $\langle n'_k n'_{k+m} \rangle$ of the projected detector noise.

We denote by n_k the detector-noise contribution prior to polynomial projection, which satisfies

$$\langle n_k \rangle = 0. \tag{23}$$

A finite segment duration induces small intersegment correlations. For stationary noise, these scale as

$$\frac{\langle n_k n_{k+m} \rangle}{\langle n_k^2 \rangle} = \mathcal{O}\left(\frac{1}{fmT_{\mathrm{seg}}}\right), \qquad (m \geq 1). \tag{24}$$

These correlations are negligible for $fT_{\mathrm{seg}} \gg 1$, and we adopt a white-noise approximation at the segment level

$$\langle n_k n_{k+m} \rangle \simeq \sigma_n^2 \delta_{m0}. \tag{25}$$

From Eq. (12), the variance σ_n^2 is set by the signal-to-noise ratio ρ_{seg} accumulated within a single segment. Using a phase estimator constructed from a single quadrature of the matched-filter output, we estimate

$$\sigma_n^2 \simeq \frac{1}{2\rho_{\mathrm{seg}}^2}, \qquad \rho_{\mathrm{seg}} = \rho_{\mathrm{tot}} \sqrt{\frac{T_{\mathrm{seg}}}{T_{\mathrm{obs}}}}. \tag{26}$$

For the fiducial model adopted throughout this work, we take $\rho_{\mathrm{tot}} = 100$ for $T_{\mathrm{obs}} = 4$ yr and a default segment duration $T_{\mathrm{seg}} = 20$ days, corresponding to $\rho_{\mathrm{seg}} \simeq 10$ and $N \simeq 70$. These values are introduced only to characterize the scaling of the noise amplitude and do not enter the formal derivations below.

We now consider the effect of polynomial phase fitting on the detector noise n_k. As shown in Sec. II, the associated projection acts linearly on the segment-level quantities,

$$\boldsymbol{n}' = P\boldsymbol{n}, \tag{27}$$

where P denotes the projection operator onto the subspace orthogonal to the polynomial phase model. The operator P is symmetric and idempotent ($P^{\mathsf{T}} = P$ and $P^2 = P$). Assuming the preprojection covariance (25), the covariance of the projected detector noise is

$$\langle n'_k n'_{k+m} \rangle = \sigma_n^2 P_{k,k+m}. \tag{28}$$

For a polynomial model of fixed order applied to N segments, the diagonal elements satisfy $P_{kk} = 1 - \mathcal{O}(p/N)$, while the off diagonal elements are suppressed as

$$P_{k,k+m} = \mathcal{O}(p/N), \qquad (m \neq 0). \tag{29}$$

Details of this scaling are discussed in the Appendix.

We conclude that detector noise induces only weak nondiagonal correlations in the projected segment-level residuals, defining a well-controlled null hypothesis for the nondiagonal correlation analysis developed in the following section.

B. Intrinsic phase fluctuation and its correlation

We now turn to the covariance $\langle s'_k s'_{k+m} \rangle$ of the projected intrinsic fluctuation.

Before the projection, we assume that the intrinsic phase fluctuation has vanishing mean,

$$\langle s_k \rangle = 0, \tag{30}$$

and is statistically stationary across segments. We also define

$$\langle s_k^2 \rangle = \sigma_s^2. \tag{31}$$

Their second-order statistics are generally characterized by the lag correlation function

$$C_m \equiv \langle s_k s_{k+m} \rangle, \tag{32}$$

which depends only on the separation m between segments.

To characterize the temporal extent of the intrinsic correlations, we introduce a correlation timescale $\tau_{\rm int}$. In terms of the segment lag m, this corresponds to an effective correlation length

$$m_{\rm int} \sim \frac{\tau_{\rm int}}{T_{\rm seg}}. \tag{33}$$

As a working approximation, we expect

$$C_m \sim C_0 = \sigma_s^2 \quad \text{for } m \lesssim m_{\rm int}, \tag{34}$$

while C_m decays for $m \gg m_{\rm int}$. No specific functional form for this decay is assumed. This provides a model-independent characterization of the range over which intrinsic phase fluctuation exhibits nondiagonal correlations.

We next consider the effect of the polynomial phase fitting on s_k. As presented in Eq. (18), we have

$$\boldsymbol{s}' = P\boldsymbol{s}. \tag{35}$$

The correlation function of the projected intrinsic fluctuation is therefore given by

$$\langle s'_k s'_{k+m}\rangle = \sum_{i,j} P_{ki} P_{k+m,j} \langle s_i s_j\rangle, \tag{36}$$

which may be written schematically, using stationarity, as

$$\langle s'_k s'_{k+m}\rangle = (PCP)_{k,k+m}, \tag{37}$$

where C denotes the covariance matrix with elements $C_{ij} = C_{|i-j|}$.

The projection removes only those components of the intrinsic fluctuation that are degenerate with the low-order polynomial phase evolution over the full observation time $T_{\rm obs}$. It therefore modifies the correlation structure on scales $\lesssim\tau_{\rm int}$ only weakly in the regime $\tau_{\rm int} \ll T_{\rm obs}$, as illustrated in the Appendix for a representative Ornstein-Uhlenbeck process [24]. We therefore approximate

$$\langle s'_k s'_{k+m}\rangle \sim C_m \sim C_0 = \sigma_s^2, \tag{38}$$

for lags $m \lesssim m_{\rm int}$. This is in contrast to the nearly diagonal structure of the projected detector noise [cf. Eq. (28)].

Even if intrinsic phase fluctuation is subdominant to detector noise at the level of individual segments, $\sigma_s \ll \sigma_n$, their correlated nature allows nondiagonal statistics to accumulate contributions over $\mathcal{O}(m_{\rm int})$ lags. This motivates the use of the nondiagonal correlation statistic introduced in the next section.

IV. NONDIAGONAL CORRELATION STATISTIC

In this section, we introduce a simple quadratic statistic Q designed to probe intrinsic stochastic phase fluctuation through its temporal correlation.

A. Definition of the statistic

We build on the segmented phase estimator expressed as

$$x_k \simeq n'_k + s'_k, \tag{39}$$

where n'_k and s'_k denote the detector noise and intrinsic stochastic contributions after polynomial phase projection.

Because $\langle x_k\rangle = 0$, linear statistics of x_k cannot probe intrinsic phase fluctuation. The intrinsic contributions s'_k instead manifest themselves in intersegment two-point functions. We therefore construct quadratic combinations of different time segments to accumulate short-lag correlations, while suppressing the nearly diagonal detector-noise component n'_k.

To make the scaling structure explicit, we adopt a simple top-hat weighting scheme and define

$$Q = \sum_{m=1}^{M} \sum_{k=1}^{N-m} x_k x_{k+m}, \tag{40}$$

where N is the total number of segments and M is the maximum lag included. The corresponding accumulation timescale is

$$\tau_2 \equiv M T_{\rm seg}. \tag{41}$$

B. Noise baseline

Under the noise-only hypothesis ($x_k = n'_k$), the expectation value becomes

$$\langle Q\rangle_n = \sum_{m=1}^{M} \sum_{k=1}^{N-m} \langle n'_k n'_{k+m}\rangle. \tag{42}$$

As discussed in Sec. III A, the off diagonal correlations of the projected detector noise are suppressed by $\mathcal{O}(1/N)$,

$$\langle n'_k n'_{k+m}\rangle = \sigma_n^2 P_{k,k+m} = \mathcal{O}\left(\frac{p\sigma_n^2}{N}\right). \tag{43}$$

Summing over k yields

$$\langle Q\rangle_n \sim pM\sigma_n^2, \tag{44}$$

which is much smaller than the statistical fluctuation $\sqrt{{\rm Var}_n(Q)}$ [see Eq. (47) below] for $pM \ll N$. Below we approximate

$$\langle Q\rangle_n \simeq 0 \tag{45}$$

at leading order.

The variance under the noise-only hypothesis is

$$\mathrm{Var}_n(Q) = \sum_{m=1}^{M}\sum_{k=1}^{N-m}\sum_{m'=1}^{M}\sum_{k'=1}^{N-m'} \langle n'_k n'_{k+m} n'_{k'} n'_{k'+m'} \rangle. \quad (46)$$

Assuming effective independence between distinct segments at leading order, the four-point function reduces to products of two-point functions, yielding

$$\mathrm{Var}_n(Q) \sim NM\sigma_n^4, \quad (47)$$

up to factors of order unity.

Projection-induced correlations modify this result only at relative order $\mathcal{O}(pM/N)$ and are neglected at leading order.

C. Expectation value from intrinsic correlations

Next, we consider the contribution of the intrinsic component s'_k, based on Eq. (38). For the maximum lag $M \lesssim m_{\mathrm{int}}$, the expectation value scales as

$$\langle Q \rangle = \sum_{m=1}^{M}\sum_{k=1}^{N-m} C_m \sim NM\sigma_s^2. \quad (48)$$

Even for $\sigma_s \ll \sigma_n$ at the segment level, the coherent accumulation over NM pairs can enhance the signal.

D. Signal-to-noise ratio and scaling

We now combine the results of the previous two subsections in the regime $\tau_2 \lesssim \tau_{\mathrm{int}}$ (equivalently $M \lesssim m_{\mathrm{int}}$). We define the signal-to-noise ratio of the statistic Q as

$$\mathrm{SN}_Q \equiv \frac{\langle Q \rangle}{\sqrt{\mathrm{Var}_n(Q)}}. \quad (49)$$

With the leading-order scalings $\langle Q \rangle \sim NM\sigma_s^2$ and $\mathrm{Var}_n(Q) \sim NM\sigma_n^4$, we obtain

$$\mathrm{SN}_Q \sim \sqrt{NM}\frac{\sigma_s^2}{\sigma_n^2}, \quad (50)$$

up to factors of order unity.

To make the scaling in Eq. (50) explicit in terms of observational parameters, we write

$$N = \frac{T_{\mathrm{obs}}}{T_{\mathrm{seg}}}, \qquad M = \frac{\tau_2}{T_{\mathrm{seg}}}, \quad (51)$$

where T_{obs} is the total observation time, T_{seg} the segment duration, and τ_2 the maximum accumulation timescale of the statistic.

To proceed, we apply the following relations:

$$\sigma_n^2 \simeq \frac{1}{2\rho_{\mathrm{seg}}^2}, \qquad \rho_{\mathrm{seg}}^2 \simeq \Gamma T_{\mathrm{seg}}, \quad (52)$$

where Γ denotes the accumulation rate of signal-to-noise of the original DWD signal presented in Eq. (2). The total coherent signal-to-noise ratio satisfies

$$\rho_{\mathrm{tot}}^2 \simeq \Gamma T_{\mathrm{obs}}. \quad (53)$$

Substituting these relations into Eq. (50), we obtain

$$\mathrm{SN}_Q \sim \sqrt{T_{\mathrm{obs}}\tau_2}\Gamma\sigma_s^2 \sim \rho_{\mathrm{tot}}^2\sigma_s^2\sqrt{\frac{\tau_2}{T_{\mathrm{obs}}}}, \quad (54)$$

up to numerical factors of order unity. Strictly speaking, intrinsic phase fluctuation $s(t)$ reduces the coherent matched-filter signal-to-noise ratio ρ_{tot} at order σ_s^2. In the small-fluctuation regime considered here, this correction is subleading and can be neglected when deriving the scaling relations below.

An important feature of Eq. (54) is the absence of explicit dependence on T_{seg}. Decreasing T_{seg} increases the number MN of contributing segment pairs, but simultaneously enlarges the variance σ_n of each segment-level estimator, leading to a cancellation at leading order.

Accordingly, the method does not rely on individually significant segment-level detections. What is required is a sufficiently large global matched-filter signal-to-noise ratio ρ_{tot} accumulated over the full observation time T_{obs}.

Realistic LISA data streams will not be perfectly continuous, and data gaps modify the above idealized scaling through the observing window. The definition of the segment-level estimator in Eq. (8) can be generalized by evaluating the inner products with the actual observing window within each segment. In this case, gaps reduce the effective signal-to-noise ratio of the affected segments and lead to nonuniform segment weights. At the level of the quadratic statistic, the uniform sum in Eq. (40) should be replaced by a weighted sum over available segment pairs. Short or randomly distributed gaps mainly reduce the effective number of contributing pairs, whereas long or regularly spaced gaps can introduce a nontrivial lag dependence in the pair count. In practical applications, the gap-free factor NM should therefore be replaced by the effective number of weighted pairs, and the variance of Q should be calibrated using the actual observing window.

E. Dependence on the intrinsic correlation time

The lag dependence of Q directly probes the intrinsic correlation time τ_{int}. For $\tau_2 \lesssim \tau_{\mathrm{int}}$, intrinsic contributions add coherently, yielding $\langle Q \rangle \propto \tau_2$. Once $\tau_2 \gtrsim \tau_{\mathrm{int}}$, correlations no longer persist over the full range of lags, and the growth of $\langle Q \rangle$ saturates. The onset of this saturation therefore provides an empirical estimate of $\tau_{\rm int}$.

While the signal saturates beyond $\tau_{\rm int}$, the noise variance continues to increase with the number of included pairs, $\mathrm{Var}_n(Q) \propto NM$. As a result, the signal-to-noise ratio SN_Q is maximized around $\tau_2 \simeq \tau_{\rm int}$. Using Eq. (54) with $\tau_2 = \tau_{\rm int}$, we obtain

$$\mathrm{SN}_{Q,\max} \sim \rho_{\rm tot}^2 \sigma_s^2 \sqrt{\frac{\tau_{\rm int}}{T_{\rm obs}}}. \tag{55}$$

The amplitude σ_s can be estimated from the measured magnitude of $\langle Q \rangle$, given the known values of N and M.

For the two parameters $\tau_{\rm int}$ and σ_s, a rough estimate of the attainable precision may be obtained by comparing the expected signal amplitude with the statistical fluctuation of Q. For an order-of-magnitude estimation, this gives

$$\frac{\delta\tau_{\rm int}}{\tau_{\rm int}} \sim \frac{\delta\sigma_s^2}{\sigma_s^2} \sim \mathrm{SN}_{Q,\max}^{-1}. \tag{56}$$

For illustration, let us consider the fiducial system with $T_{\rm obs} = 4$ yr and $\rho_{\rm tot} = 100$. The above scaling then gives

$$\mathrm{SN}_{Q,\max} \sim 35 \left(\frac{\rho_{\rm tot}}{100}\right)^2 \left(\frac{\sigma_s}{0.1}\right)^2 \left(\frac{\tau_{\rm int}}{0.5\ \mathrm{yr}}\right)^{1/2} \left(\frac{T_{\rm obs}}{4\ \mathrm{yr}}\right)^{-1/2}, \tag{57}$$

indicating that even modest intrinsic phase fluctuation can produce a statistically significant nondiagonal signal when correlations persist over long timescales. The numerical choice $\tau_{\rm int} = 0.5$ yr in this estimate is intended as an illustrative correlation timescale in the simplified response model. It should not be interpreted as implying that annual-response effects are negligible near this timescale, especially when the observing baseline spans only a few annual cycles.

V. DISCUSSION

We now discuss the relation of the proposed statistic to existing methods and its possible extensions.

A. Relation to pulsar timing analyses

The analysis presented here is conceptually related to studies of intrinsic noise processes in pulsar timing, where a phaselike observable is tracked over long timescales and deviations from a low-order polynomial model are analyzed through timing residuals (e.g., Refs. [14,17,25]). In both contexts, the essential task is to identify temporally correlated fluctuation in phase residuals obtained after fitting a smooth deterministic phase evolution.

B. Relation to stochastic background analyses

The nondiagonal correlation statistic introduced here is structurally analogous to the correlation analysis for stochastic GW background searches [26,27]. In both cases, correlated components are extracted through quadratic combinations of data characterized by a nontrivial two-point function. A key distinction is that the present analysis forms correlations between different times within a single data stream, rather than between distinct detectors at the same time.

From this perspective, combinations of noise-independent detector channels, as extensively studied in stochastic background analyses, are naturally compatible with the present framework. Examples include combinations of the multiple time-delay interferometry variables within LISA, as well as cross-mission networks such as LISA-Taiji.

The same viewpoint also suggests a population-level implication. If intrinsic phase fluctuations are present in many DWDs, subtraction with smooth deterministic templates would leave residuals that are not solely due to ordinary parameter-estimation errors. Even after the best-fit deterministic parameters are removed, the unmodeled stochastic component can remain as a source-origin residual with temporal correlations inherited from the underlying phase fluctuation. Such residuals could contribute to the postsubtraction foreground, although quantifying this effect would require a dedicated population-level simulation.

C. Sensitivity to general phase modulations

Although the present analysis has focused on internal processes for isolated DWDs, the same framework can serve as a screening tool for more general phase modulations. Weak perturbations, such as those induced by a third body (e.g., Refs. [28,29]) or other external influences, may generate small but temporally correlated deviations from a smooth phase evolution.

For a well-specified deterministic perturbation, a dedicated coherent template fit would ultimately provide the most powerful detection and parameter-estimation method. The role of the present statistic is complementary: it tests, in a model-independent way, whether the residuals left after the baseline deterministic phase fit contain nondiagonal temporal correlations that justify a more detailed model extension. In this sense, a significant detection of correlated phase residuals would identify systems that warrant subsequent residual-space analyses based on physical templates or covariance models.

D. Synergies with electromagnetic observations

The analysis presented here relies exclusively on GW data to probe stochastic features in orbital phase evolution. Electromagnetic observations provide complementary information, and joint interpretation may offer additional insight into the underlying astrophysical processes. They can also help control deterministic detector-response effects. In particular, the dominant annual Doppler phase modulation is largely determined by the sky position of the binary and the known orbital motion of LISA. For optically identified binaries with accurately measured sky positions, this component can therefore be modeled with high precision, reducing its degeneracy with source-side phase variations. In favorable systems, electromagnetic timing or photometric monitoring may also provide an independent reference for interpreting correlated GW phase residuals.

E. Applicability to other long-lived compact binaries

The framework is not limited to DWDs. Any long-lived compact binary with a coherently trackable GW phase may be analyzed in a similar manner. Examples include early inspiral stellar-mass black holes (e.g., Ref. [30]) and neutron-star–white-dwarf systems [1]. A detailed assessment of correlated phase fluctuation in these systems is left for future work.

F. Modeling scope and outlook

The present analysis isolates the leading nondiagonal correlation structure induced by stochastic phase fluctuation. More refined treatments could incorporate explicit covariance modeling or embed the same structure within a Bayesian inference framework, as commonly done in pulsar timing analyses and stochastic background searches. A full demonstration with simulated LISA data would be a natural next step. Such an analysis would have to include the time-dependent LISA response, parameter covariance, data gaps, and residual foreground or source-subtraction effects. We leave this more complete implementation for future work, while the present paper provides the analytic baseline for the corresponding residual-correlation statistic.

VI. SUMMARY

We present a minimal diagnostic framework for intrinsic stochastic phase fluctuation in GW signals from DWDs, constructed from time correlations of phase residuals.

Dividing the data into short segments, we form a quadratic intersegment correlation statistic. Analytic expressions for its expectation value and variance show that the resulting signal-to-noise ratio is independent of the chosen segment duration and scales with the total observation time and the effective correlation time.

These results clarify how weak but temporally correlated phase fluctuation can accumulate coherently over long observations. They provide a transparent baseline for assessing the detectability of such effects in nearly monochromatic GW signals from long-lived compact binaries.

ACKNOWLEDGMENTS

This work was supported by JSPS KAKENHI Grant Nos. JP23K03385 and JP26H00834.

DATA AVAILABILITY

The data that support the findings of this article are not publicly available. The data are available from the authors upon reasonable request.

APPENDIX: EFFECTS OF POLYNOMIAL PHASE FITTING

This appendix summarizes the statistical effect of polynomial phase fitting on segment-level detector noise n_k and intrinsic phase fluctuation s_k.

Although both are acted upon by the same linear projection operator P, their statistical responses differ. For initially uncorrelated detector noise, the induced correlations are weak, and the variance reduction is small. For intrinsically correlated phase fluctuation, the impact of the projection depends on the ratio $\tau_{\rm int}/T_{\rm obs}$.

1. Detector noise

Before phase fitting, the segment-level noise sequence n_k is assumed to be stationary, zero mean, and uncorrelated,

$$\langle n_k\rangle = 0, \qquad \langle n_k n_l\rangle = \sigma_n^2\delta_{kl}, \tag{A1}$$

where σ_n^2 denotes the variance per segment.

Polynomial phase fitting acts on the discretized noise through the linear projection operator P introduced in the main text,

$$\boldsymbol{n}' = P\boldsymbol{n}, \tag{A2}$$

with $P^{\mathsf{T}} = P = P^2$. The covariance matrix of the projected noise is therefore

$$\langle \boldsymbol{n}'\boldsymbol{n}'^{\mathsf{T}}\rangle = \sigma_n^2 P. \tag{A3}$$

Polynomial fitting induces weak intersegment correlations through the off diagonal elements of P. The mean variance reduction is quantified by

$$R_n \equiv \frac{\sum_{k=1}^{N}\langle (n_k')^2\rangle}{\sum_{k=1}^{N}\langle n_k^2\rangle} = \frac{1}{N}\mathrm{Tr}(P), \tag{A4}$$

where N is the number of segments.

For a degree-p polynomial fit,

$$\mathrm{Tr}(P) = N-(p+1), \tag{A5}$$

implying

$$R_n = 1-\frac{p+1}{N}. \tag{A6}$$

For $k \neq l$, the induced correlations satisfy

$$\langle n'_k n'_l \rangle = \mathcal{O}\left(\frac{p+1}{N}\right)\langle n'^2_k \rangle, \tag{A7}$$

reflecting the fact that $P_{kl} = \mathcal{O}((p+1)/N)$ while $P_{kk} = 1 - \mathcal{O}((p+1)/N)$.

Polynomial fitting induces $\mathcal{O}(1/N)$ long-range correlations in the discretized noise.

2. Intrinsic phase fluctuation

We next consider intrinsic stochastic phase fluctuation. The fitting again acts through the same projection operator,

$$\boldsymbol{s}' = P\boldsymbol{s}, \tag{A8}$$

but the resulting impact depends on the temporal covariance of the intrinsic process. We assume $\langle s_k \rangle = 0$ and denote

$$\langle s_k s_{k+m} \rangle = C_{|m|}. \tag{A9}$$

After projection, the covariance becomes

$$\langle \boldsymbol{s}' \boldsymbol{s}'^{\mathsf{T}} \rangle = PCP, \tag{A10}$$

where $C_{ij} = C_{|i-j|}$. Unlike the detector-noise case, the suppression therefore depends explicitly on the structure of C.

To quantify the suppression, we define

$$R_s \equiv \frac{\sum_{k=1}^{N} \langle (s'_k)^2 \rangle}{\sum_{k=1}^{N} \langle s_k^2 \rangle} = \frac{\mathrm{Tr}(PCP)}{\mathrm{Tr}(C)}, \tag{A11}$$

which depends on the temporal structure of C.

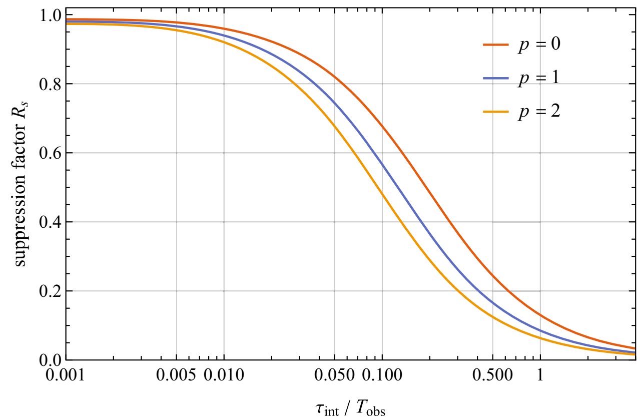

FIG. 1. Suppression factor R_s as a function of $\tau_{\rm int}/T_{\rm obs}$. Short-memory fluctuation ($\tau_{\rm int} \ll T_{\rm obs}$) is weakly affected, whereas long-memory fluctuation is increasingly suppressed.

As an illustration, we adopt a discrete Ornstein–Uhlenbeck model with

$$C_{ij} = \sigma_s^2 \exp\left(-\frac{|i-j|T_{\rm seg}}{\tau_{\rm int}}\right), \tag{A12}$$

where $\tau_{\rm int}$ is the intrinsic correlation time. This example is used only for illustration.

For this model, R_s can be evaluated numerically as a function of $\tau_{\rm int}/T_{\rm obs}$ and p. Figure 1 shows that $R_s \simeq 1$ for $\tau_{\rm int} \ll T_{\rm obs}$, whereas long-memory fluctuation is increasingly suppressed. Since polynomial fitting is performed over the full observation span, this qualitative behavior is physically expected and should hold quite generally, without relying on the specific form of the intrinsic correlation function.

[1] P. Amaro-Seoane *et al.* (LISA Collaboration), Living Rev. Relativity **26**, 2 (2023).
[2] W.-R. Hu and Y.-L. Wu, Natl. Sci. Rev. **4**, 685 (2017).
[3] J. Luo, L.-S. Chen, H.-Z. Duan, Y.-G. Gong, S. Hu, J. Ji, Q. Liu, J. Mei, V. Milyukov, M. Sazhin *et al.*, Classical Quantum Gravity **33**, 035010 (2016).
[4] V. Korol, E. M. Rossi, P. J. Groot, G. Nelemans, S. Toonen, and A. G. A. Brown, Mon. Not. R. Astron. Soc. **470**, 1894 (2017).
[5] L. Blanchet, Living Rev. Relativity **17**, 2 (2014).
[6] E. Poisson and C. M. Will, *Gravity: Newtonian, Post-Newtonian, Relativistic* (Cambridge University Press, Cambridge, England, 2014).
[7] M. Maggiore, *Gravitational Waves* (Oxford University Press, New York, 2008), Vol. 2.
[8] R. Takahashi and N. Seto, Astrophys. J. **575**, 1030 (2002).
[9] V. Gokhale, X. Peng, and J. Frank, Astrophys. J. **655**, 1010 (2007).
[10] J. Fuller and D. Lai, Mon. Not. R. Astron. Soc. **420**, 3126 (2012).
[11] T. E. Strohmayer, Astrophys. J. Lett. **912**, L8 (2021).
[12] T. E. Strohmayer, Astrophys. J. Lett. **627**, L53 (2005).
[13] R. T. Edwards, G. B. Hobbs, and R. N. Manchester, Mon. Not. R. Astron. Soc. **372**, 1549 (2006).
[14] W. Coles, G. Hobbs, D. J. Champion, R. N. Manchester, and J. P. W. Verbiest, Mon. Not. R. Astron. Soc. **418**, 2167 (2011).
[15] G. B. Hobbs, R. T. Edwards, and R. N. Manchester, Mon. Not. R. Astron. Soc. **369**, 655 (2006).
[16] R. W. Hellings and G. S. Downs, Astrophys. J. Lett. **265**, L39 (1983).

[17] R. van Haasteren and Y. Levin, Mon. Not. R. Astron. Soc. **428**, 2489 (2013).
[18] C. Cutler, Phys. Rev. D **57**, 7089 (1998).
[19] P. Jaranowski, A. Królak, and B. F. Schutz, Phys. Rev. D **58**, 063001 (1998).
[20] C. Cutler and M. Vallisneri, Phys. Rev. D **76**, 104018 (2007).
[21] C. R. Rao, *Linear Statistical Inference and Its Applications*, 2nd ed. (John Wiley & Sons, New York, 1973).
[22] G. A. F. Seber and A. J. Lee, *Linear Regression Analysis*, 2nd ed. (John Wiley & Sons, Hoboken, NJ, 2003).
[23] In a real-valued formulation, this operation is equivalent to taking an inner product with a template whose phase is shifted by $\pi/2$ relative to the original template h, i.e., projecting onto the quadrature component that is orthogonal to h in the real signal space.
[24] C. W. Gardiner, *Stochastic Methods* (Springer, New York, 2009).
[25] L. Lentati, P. Alexander, M. P. Hobson, S. R. Taylor, and J. R. Gair, Phys. Rev. D **87**, 104021 (2013).
[26] B. Allen and J. D. Romano, Phys. Rev. D **59**, 102001 (1999).
[27] J. D. Romano and N. J. Cornish, Living Rev. Relativity **20**, 2 (2017).
[28] N. Seto, Astrophys. J. Lett. **677**, L55 (2008).
[29] N. Tamanini and C. Danielski, Nat. Astron. **3**, 858 (2019).
[30] N. Seto and K. Kyutoku, Mon. Not. R. Astron. Soc. **514**, 4669 (2022).